

On the single photon background to ν_e appearance at MiniBooNE

Richard J. Hill*

*Enrico Fermi Institute and Department of Physics
The University of Chicago, Chicago, Illinois, 60637, USA*

(Dated: September 22, 2021)

Neglected single photon processes are fit to an excess of electron-like events observed in a predominantly ν_μ beam at MiniBooNE. Predictions are given for analogous events in antineutrino mode.

PACS numbers: 12.38.Qk, 12.39.Fe, 13.15.+g,

I. INTRODUCTION

The MiniBooNE experiment was designed to test the indication of a $\bar{\nu}_\mu \rightarrow \bar{\nu}_e$ oscillation signal at LSND [1, 2]. MiniBooNE data for ν_e appearance in a ν_μ beam [3], when restricted to the range of 475 – 1250 MeV reconstructed neutrino energy, refute a simple two-neutrino oscillation interpretation for the LSND signal. However, the results indicate an excess of signal-like events at low energy, which has persisted at the 3σ level after various refinements to the analysis [4]. First results from MiniBooNE for $\bar{\nu}_e$ appearance in a $\bar{\nu}_\mu$ beam do not show a significant excess [5], but are inconclusive with respect to the LSND signal.

Because electromagnetic showers instigated by electrons and photons are not distinguishable at MiniBooNE, neutral current events producing single photons are an irreducible background to the charged current $\nu_e n \rightarrow e^- p$ signal. This note presents flux-averaged cross sections for the dominant sources of single-photon backgrounds, some of which were not incorporated in the MiniBooNE analysis. These standard model processes must be well-understood and accounted for before appealing to more exotic interpretations of the electron-like signal.

II. SINGLE PHOTON PROCESSES

The ~ 1 GeV energy range is unfortunately not well suited to precise analytic results, since there is no obvious small expansion parameter for this regime of QCD [21]. At low energy, contributions to the process of interest can be tabulated in the rigorous language of a chiral lagrangian expansion. Extrapolation to moderate energy can then be performed by explicitly including the lowest-lying resonances in each channel, and adopting phenomenological form factors to mimic the effects of higher resonances. This methodology was discussed in detail in [6]. This study was motivated by the search for low-energy remnants of the baryon current anomaly,

such as the coherent coupling of weak and electromagnetic currents to baryon density [7][22].

In terms of the chiral lagrangian expansion, the production of single photons in neutrino scattering on nucleons begins at order $1/M$ [23]. The $1/M$ contributions represent offshell intermediate nucleon states or Compton-like scattering, including bremsstrahlung corrections to elastic scattering. At the next order there appears a term that derives from s -channel $\Delta(1232)$ production and t -channel $\omega(780)$ exchange. Exchange of π^0 in the t -channel is naively of similar size but is suppressed by an amplitude factor $1 - 4\sin^2\theta_W \approx 0.08$ [8]. Similarly, exchange of isovector $\rho(770)$ is suppressed relative to isoscalar $\omega(780)$ by a factor $\sim (1/3)^2$ from quark counting rules. The Δ and ω contributions are spin-independent interactions at low energy, and can also give rise to coherent scattering on compound nuclei such as ^{12}C in the MiniBooNE detector. The coherent contribution from bremsstrahlung emission on the nucleus is numerically small.

In what follows, the coherent bremsstrahlung process, and the incoherent π^0 and ρ^0 processes, are neglected. The remaining contributions are computed using the parameter values and form factor models from [6] and the published MiniBooNE fluxes in both neutrino and antineutrino modes [9]. Only the incoherent Δ contribution was studied in the MiniBooNE analysis, with normalization constrained by comparison to observed π^0 production and a model of final state interactions. The result of this procedure is compared to a direct calculation of the incoherent Δ contribution. Nuclear effects and other uncertainties are briefly discussed.

III. MINIBOONE NEUTRINO CROSS SECTIONS

Figure 1 displays flux-integrated cross sections, presented as events per MeV of reconstructed neutrino energy [24]. The normalization corresponds to a detector mass of $800 \times 10^6 g$, and 6.46×10^{20} protons on target for the updated analysis of ν_e charged current quasi-elastic (CCQE) events in a primarily ν_μ beam [4]. A cut $E_\gamma \geq 140$ MeV is placed on the photon energy, in accordance with the experimental selection.

*Electronic address: richardhill@uchicago.edu

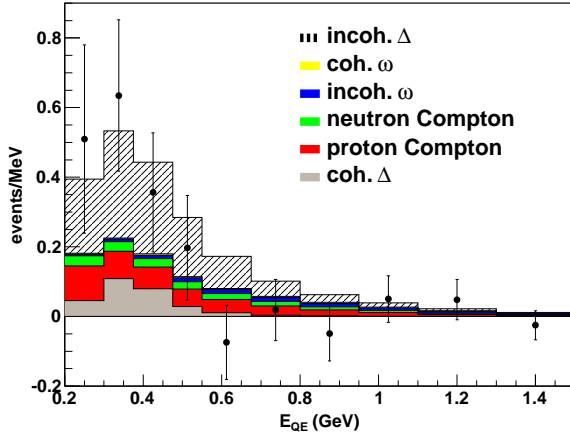


FIG. 1: Single-photon events at MiniBooNE for 6.46×10^{20} protons on target in neutrino mode. A 25% efficiency is assumed. The hatched line represents the difference between the direct calculation and MiniBooNE π^0 -constrained incoherent $\Delta \rightarrow N\gamma$ background. Data points correspond to the excess events reported in [4], Fig. 2.

To compare to the MiniBooNE data in the absence of a dedicated efficiency analysis, the number of events has been multiplied by an efficiency factor of 25% and detector resolution/smearing effects have been neglected. For comparison, the original MiniBooNE analysis quotes an efficiency of $30.6 \pm 1.4\%$ for reconstructing signal-like ν_e CCQE events [3]. As can be seen from Table I, after selection cuts the efficiency for events with similar signatures, $\nu_\mu e^- \rightarrow \nu_\mu e^-$ and $\nu_e n \rightarrow e^- p$, fall in the range 20 – 30% [25]. It can also be seen from this table that the direct estimate of the number of single photon events mediated by $\Delta(1232)$ is larger than the π^0 -constrained background estimate of MiniBooNE by a factor ≈ 2 [26]. The effects of a larger incoherent $\Delta \rightarrow N\gamma$ background are illustrated by the hatched area in Fig. 1, computed by adding 0.5 times the direct estimate (i.e., effectively doubling the MiniBooNE background). Under the assumption of a constant 25% efficiency, the fit of these additional single-photon events to the MiniBooNE excess yields $\chi^2 = 10.3$ for 10 d.o.f. Theoretical errors are discussed at the end of this note and have not been included in the fit. Assuming a lower 20% efficiency and taking the difference between the estimates of $\Delta \rightarrow N\gamma$ events from the table, the remaining excess would be 15 ± 26 , 23 ± 25 and -47 ± 36 in the 200 – 300, 300 – 475 and 475 – 1250 MeV bins, respectively. If no additional incoherent $\Delta \rightarrow N\gamma$ events are included, these numbers become 29 ± 26 , 55 ± 25 and -9 ± 36 .

The most significant excess in the updated MiniBooNE analysis occurred in the $E_{QE} = 300 - 475$ MeV bin. The distributions in reconstructed Q^2 [27], and cosine of the angle, $\cos\theta$, of the electromagnetic shower with respect to the beam direction, are displayed for this energy range

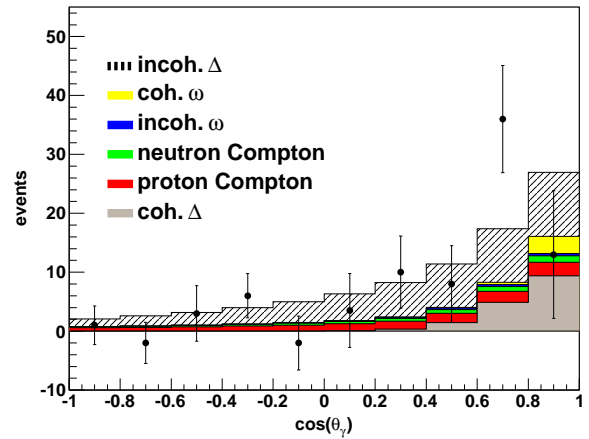
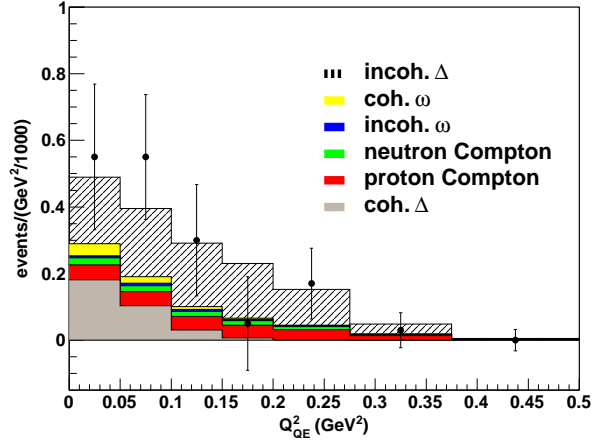


FIG. 2: Distributions in Q^2_{QE} and $\cos\theta$ for the events displayed in Figure 1 for $E_{QE} = 300 - 475$ MeV. Data points correspond to Figs. 4 and 5 of [4].

TABLE I: Single photon and other backgrounds for MiniBooNE ν -mode in ranges of E_{QE} . Ranges in square brackets are the result of applying a 20 – 30% efficiency correction.

process	200-300	300-475	475-1250
1γ , non- Δ	85[17 – 26]	151[30, 45]	159[32, 48]
$\Delta \rightarrow N\gamma$	170[34 – 51]	394[79 – 118]	285[57 – 86]
$\nu_\mu e \rightarrow \nu_\mu e$	14[2.7 – 4.1]	20[4.0 – 5.9]	40[7.9 – 12]
$\nu_e n \rightarrow ep$	100[20 – 30]	303[61 – 91]	1392[278 – 418]
MB excess	45.2 ± 26.0	83.7 ± 24.5	22.1 ± 35.7
MB $\Delta \rightarrow N\gamma$	19.5	47.5	19.4
MB $\nu_\mu e \rightarrow \nu_\mu e$	6.1	4.3	6.4
MB $\nu_e n \rightarrow ep$	19	62	249

in Figure 2. The normalization assumes an energy- and angle-independent efficiency of 25%, and includes 0.5 times the incoherent $\Delta \rightarrow N\gamma$ background as in Figure 1. A χ^2 fit yields 10.9/10 d.o.f. for $\cos\theta$ and 2.6/7 d.o.f. for Q^2_{QE} .

Note that in the accounting method here, it does not

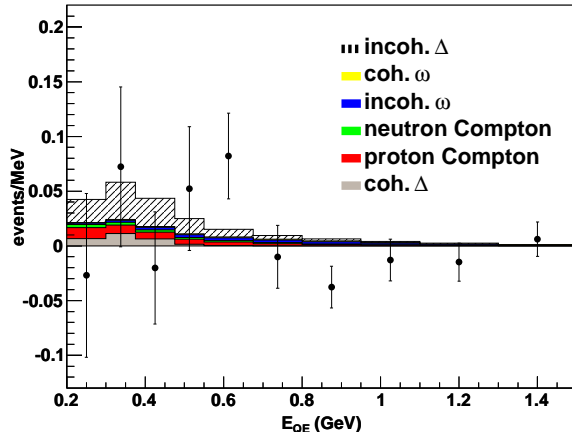


FIG. 3: Comparison of single photon events to MiniBooNE data with other backgrounds subtracted in antineutrino mode.

matter whether the MiniBooNE $\Delta \rightarrow N\gamma$ background estimate represents just the incoherent, or the sum of incoherent plus coherent processes. In the latter case, the difference between the π^0 -constrained background and the direct estimates given here would be larger; the “ Δ ” and “coherent Δ ” regions in the figures would contribute different amounts but with the same total.

From the estimates presented here, it may be difficult to extract the coherent component from other backgrounds. Doing so would represent the first signal for coherent single photon production by the weak neutral current above the nuclear scale [28].

IV. MINIBOONE ANTINEUTRINO CROSS SECTIONS

The above procedure may be repeated for antineutrinos. Figure 3 displays flux-integrated cross sections normalized according to 3.39×10^{20} protons on target from the search for $\bar{\nu}_e$ CCQE events in a primarily $\bar{\nu}_\mu$ beam [5]. A cut $E_\gamma \geq 140$ MeV is applied, and a 25% efficiency has been assumed, in accordance with a comparison to MiniBooNE backgrounds in Table II [29]. Again, the direct estimate of $\Delta \rightarrow N\gamma$ events is ≈ 2 times larger than the MiniBooNE estimate; the difference is illustrated in the figure by including 0.5 times the direct estimate for these events. The resulting fit for the E_{QE} distribution yields $\chi^2 = 13.3$ for 10 d.o.f. Assuming a 20% efficiency and taking the difference between the estimates of $\Delta \rightarrow N\gamma$ events from the table, the excess becomes -11.5 ± 11.7 and -2.8 ± 10.0 in the 200 – 475 and 475 – 1250 MeV bins, respectively. If no additional incoherent $\Delta \rightarrow N\gamma$ events are included, these numbers become -6.1 ± 11.7 and -0.2 ± 10.0 .

TABLE II: Single photon and other backgrounds for MiniBooNE $\bar{\nu}$ -mode in ranges of E_{QE} . Ranges in square brackets are the result of applying a 20 – 30% efficiency correction.

process	200-475	475-1250
1γ , non- Δ	28[5.6-8.4]	17[3.4-5.2]
$\Delta \rightarrow N\gamma$	58[12-17]	23[4.6-6.9]
$\bar{\nu}_e/\nu_e$ CCQE	81[16-24]	261[52-78]
MB excess	-0.5 ± 11.7	3.2 ± 10.0
MB $\Delta \rightarrow N\gamma$	6.6	2.0
MB $\bar{\nu}_e/\nu_e$ CCQE	18	43

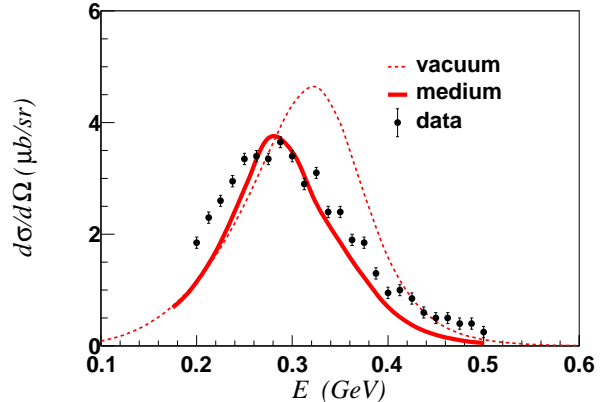


FIG. 4: Coherent photon scattering on ^{12}C mediated by Δ resonance at $\theta = 40^\circ$ ($\cos\theta = 0.766$). Dashed line is model with energy-independent width $\Gamma_\Delta = 120$ MeV. Solid line is for energy-dependent width and in-medium effects as described in text. Data is from [10].

V. NUCLEAR EFFECTS AND OTHER UNCERTAINTIES

The absence of an obvious small expansion parameter complicates error estimation for $E \sim \text{GeV}$ cross sections involving hadronic matrix elements. At the single nucleon level, the $1/N_c$ expansion of QCD motivates the assignment of $\mathcal{O}(1/N_c) \sim 30\%$ uncertainty to tree level amplitudes when all of the relevant resonances are included. Nuclear corrections induce additional uncertainty. Here we consider some of these, focusing on in-medium effects on the coherent cross section, and Fermi motion effects on the incoherent cross section.

The largest component of the coherent amplitude at low energy is due to the $\Delta(1232)$ resonance in the s channel [30]. To gauge whether the nuclear modeling for the coherent process mediated by Δ excitation gives a reasonable approximation to the true cross section, it is useful to compare to the analog process of coherent photon scattering on the same nucleus. Data from [10] at a fixed angle $\theta = 40^\circ$ is shown in Fig. 4. The dashed line in the figure shows the result of the “default” model from [6]

(with photon in place of the vector-coupled Z^0), using energy-independent width $\Gamma_\Delta = 120$ MeV. For comparison, the result of including in-medium modifications to Δ propagation and using energy-dependent width is displayed as the solid line. Here a simple model for these modifications is taken from Drechsel *et al.* [18] [31].

As the figure illustrates, the data is in better agreement with the model incorporating in-medium effects, where the cross section is somewhat reduced, and the peak shifted to smaller energy. The fit to the data can be improved by using a slightly larger vacuum width (e.g. $\Gamma_\Delta \sim 130$ MeV) and including a small nonresonant background. However, these modifications are beyond the accuracy of other approximations such as the simplified nuclear form factor and nonrelativistic reduction of the amplitude. The main point to be illustrated is that the simple model represented by the dashed line is not a gross misrepresentation of the data.

The incoherent single-photon cross sections have been calculated neglecting nuclear effects. From a comparison of the CCQE cross sections computed assuming free nucleons, and those using a relativistic Fermi gas model, the nuclear binding, Fermi motion of the initial-state nucleons, and Pauli blocking of the final state nucleons, are seen to affect the cross sections on the $\sim 10 - 15\%$ level for the relevant energies. Similarly, in-medium modification of parameters such as m_Δ , Γ_Δ should affect the cross sections at a $\sim 10 - 20\%$ level, as seen in the above example for coherent Compton scattering, or in related analyses of single pion production through the Δ resonance [32]. The effects of higher baryon resonances are small ($< 10\%$) relative to $\Delta(1232)$, based on the production cross sections below 2 GeV neutrino energy [11]. Interference effects between different photon production mechanisms (ω , Δ , Compton) have been neglected. A detailed study is beyond the scope of this work. The distinct kinematic distributions [6] suggest that interference

effects will not drastically alter the total cross sections at the energies accessible to MiniBooNE. Photons produced by rescattering of pions in the nucleus have been neglected.

The range of 30 – 50% is a subjective estimate of the total single-photon cross section uncertainty. A dedicated efficiency analysis would constrain the overall normalization error. Examination of processes such as $\nu_\mu n \rightarrow \mu^- p \gamma$ could be used to test other sources of uncertainty [33]. This process avoids complications from final-state pion interactions, but involves different linear combinations of the hadronic matrix elements than contribute to the neutral current process.

VI. SUMMARY

Neglected single photon events give a significant contribution to the MiniBooNE low-energy excess. Fits to the data also favor an enhanced resonant $\Delta \rightarrow N\gamma$ contribution (either incoherent or coherent) relative to estimates based on π^0 production. A similar enhancement is predicted by a phenomenological model calculation, and is consistent with the absence of a significant excess in the MiniBooNE antineutrino results. An enhanced coupling of the neutral weak current and electromagnetic current to baryons may have interesting astrophysical implications [7].

VII. ACKNOWLEDGEMENTS

I have benefited from discussions with M. Shaevitz, J. Conrad, G. Garvey, J. Harvey, C. Hill, G. Paz and G. Zeller. Work supported by NSF Grant 0855039.

-
- [1] C. Athanassopoulos *et al.* [LSND Collaboration], Phys. Rev. Lett. **77**, 3082 (1996) [arXiv:nucl-ex/9605003].
- [2] C. Athanassopoulos *et al.* [LSND Collaboration], Phys. Rev. Lett. **81**, 1774 (1998) [arXiv:nucl-ex/9709006].
- [3] A. A. Aguilar-Arevalo *et al.* [The MiniBooNE Collaboration], Phys. Rev. Lett. **98**, 231801 (2007) [arXiv:0704.1500 [hep-ex]].
- [4] A. A. Aguilar-Arevalo *et al.* [MiniBooNE Collaboration], Phys. Rev. Lett. **102**, 101802 (2009) [arXiv:0812.2243 [hep-ex]].
- [5] A. A. Aguilar-Arevalo *et al.*, arXiv:0904.1958 [hep-ex].
- [6] R. J. Hill, Phys. Rev. D **81**, 013008 (2010) [arXiv:0905.0291 [hep-ph]].
- [7] J. A. Harvey, C. T. Hill and R. J. Hill, Phys. Rev. Lett. **99**, 261601 (2007) [arXiv:0708.1281 [hep-ph]]. J. A. Harvey, C. T. Hill and R. J. Hill, Phys. Rev. D **77**, 085017 (2008) [arXiv:0712.1230 [hep-th]].
- [8] The $1 - 4 \sin^2 \theta_W$ factor results from a near cancellation between isoscalar and isovector components of the weak current. The cancellation is rigorously valid at low energy where the pion chiral lagrangian is valid. Avoiding the cancellation at higher energy would require dramatic violation of vector meson dominance. This possibility was considered in: J. Jenkins and T. Goldman, Phys. Rev. D **80**, 053005 (2009) [arXiv:0906.0984 [hep-ph]].
- [9] A. A. Aguilar-Arevalo *et al.* [MiniBooNE Collaboration], Phys. Rev. D **79**, 072002 (2009) [arXiv:0806.1449 [hep-ex]].
- [10] F. Wissmann *et al.*, Phys. Lett. B **335**, 119 (1994).
- [11] O. Lalakulich, E. A. Paschos and G. Piranishvili, Phys. Rev. D **74**, 014009 (2006) [arXiv:hep-ph/0602210]. T. Leitner, O. Buss, L. Alvarez-Ruso and U. Mosel, Phys. Rev. C **79**, 034601 (2009) [arXiv:0812.0587 [nucl-th]].
- [12] R. A. Smith and E. J. Moniz, Nucl. Phys. B **43**, 605 (1972) [Erratum-ibid. B **101**, 547 (1975)].
- [13] D. Rein and L. M. Sehgal, Phys. Lett. B **104**, 394 (1981) [Erratum-ibid. B **106**, 513 (1981)].
- [14] B. Armbruster *et al.* [KARMEN Collaboration], Phys.

- Lett. B **423**, 15 (1998).
- [15] H. Faissner *et al.*, Phys. Rev. Lett. **41**, 213 (1978) [Erratum-ibid. **41**, 1083 (1978)].
- [16] E. Isiksal, D. Rein and J. G. Morfin,
- [17] K. Greisen, Phys. Rev. Lett. **16**, 748 (1966); G. T. Zatspepin and V. A. Kuzmin, JETP Lett. **4**, 78 (1966) [Pisma Zh. Eksp. Teor. Fiz. **4**, 114 (1966)].
- [18] D. Drechsel, L. Tiator, S. S. Kamalov and S. N. Yang, Nucl. Phys. A **660**, 423 (1999) [arXiv:nucl-th/9906019].
- [19] T. Leitner, O. Buss, U. Mosel and L. Alvarez-Ruso, Phys. Rev. C **79**, 038501 (2009) [arXiv:0812.1787 [nucl-th]].
- [20] A. A. Aguilar-Arevalo *et al.* [MiniBooNE Collaboration], arXiv:0710.3897 [hep-ex].
- [21] The discussion can be formalized by appealing to the large N_c limit.
- [22] In terms of the baryon chiral lagrangian, the operator induced by t -channel ω exchange (considered in [7]) also receives contributions from s - and u -channel Δ . The amplitudes constructively interfere at energies $E \ll m_\omega, m_\Delta - m_N$, with Δ appearing to give the larger contribution. Further discussion, including extrapolation to larger energy and kinematic distributions for different photon production mechanisms, can be found in [6].
- [23] $M \sim m_N \sim 4\pi f_\pi \sim 1 \text{ GeV}$.
- [24] The reconstructed neutrino energy assumes charged current quasielastic scattering on a stationary nucleon to an electron final state. Neglecting the electron mass, we have $E_{QE} \equiv E_{vis}/[1 - (E_{vis}/m_N)(1 - \cos\theta)]$.
- [25] For the CCQE events, the small $\bar{\nu}_e$ contamination in the beam is neglected and the cross section is calculated in a standard relativistic Fermi gas model of Smith and Moniz [12], with model parameters $\epsilon_b = 27 \text{ MeV}$ and $k_F = 225 \text{ MeV}$.
- [26] Using the energy-dependent Breit-Wigner width gives a lower total cross section and pulls events to lower energy: with the same form factors the number of events would be 217, 363 and 175 in the 200 – 300, 300 – 475 and 475 – 1250 MeV bins, respectively. For definiteness, we focus on the “default” cross sections from [6].
- [27] The reconstructed Q^2 variable is defined, neglected electron mass, as $Q_{QE}^2 \equiv 2E_{vis}^2(1 - \cos\theta)/[1 - (E_{vis}/m_N)(1 - \cos\theta)]$.
- [28] Nuclear excitation yields coherent photon production at the $\sim \text{MeV}$ energy scale, e.g. [14]. While some hints of single photon events were discussed in previous high-energy experiments, these were not definitively isolated as being due to single photons as opposed e.g. to π^0 production with a missed photon [15, 16].
- [29] For CCQE events, the estimate includes 4/3 of the $\bar{\nu}_e$ cross section on ^{12}C to account for hydrogen (neglecting the difference between free and bound protons), as well as the ν_e cross section on ^{12}C . Cross sections are computed as in the ν_e case, using a relativistic Fermi gas model.
- [30] This process may be viewed as a “reverse coherent GZK” effect [17].
- [31] The modifications are implemented using Eqs.(25) and (26a) and Fig.5 of [18]. The complex phase ϕ discussed there has been neglected.
- [32] See e.g. [19]. In this case, the final-state interactions of the pion are intertwined with in-medium modifications to the primary vertex.
- [33] A sample of muon events with photons was isolated in [20]. J. Conrad, private communication.